Available online at www.sciencedirect.com
ScienceDirect
Bioelectrochemistry 71 (2007) 15–22
Bioelectrochemistry
www.elsevier.com/locate/bioelechem

Immobilization of laccase on gold, silver and indium tin oxide by zirconium–phosphonate–carboxylate (ZPC) coordination chemistry

M. Mazur [a], P. Krysiński [a,*], A. Michota-Kamińska [a], J. Bukowska [a], J. Rogalski [b], G.J. Blanchard [c]

[a] University of Warsaw, Department of Chemistry, 02-093 Warsaw, Pasteura 1, Poland
[b] Maria Curie-Skłodowska University, Department of Biochemistry, 20-031 Lublin, Plac Marii Curie-Skłodowskiej 3, Poland
[c] Michigan State University, Department of Chemistry, E. Lansing, MI 48824-1322, USA

Received 10 March 2006; received in revised form 2 November 2006; accepted 29 December 2006
Available online 13 January 2007

Abstract

In this paper we present a simple method allowing for stable laccase immobilization on various conducting surfaces that retains the activity of the enzyme. The strategy for laccase immobilization presented in this paper relies on Zr^{4+} ion coordination chemistry that involves $-COO^-$ terminal groups present on the protein. Using a host of techniques, including surface plasmon resonance (SPR), quartz crystal microbalance (QCM) gravimetry, atomic force microscopy (AFM), surface enhanced Raman scattering (SERS), resonance Raman scattering (RR) and electrochemical techniques, we show that laccase bound to a surface coordinatively through zirconium phosphonate/carboxylate (ZPC) functionalities forms a stable enzymatic layer with the enzyme retaining its activity to a significant extent.

Keywords: Zirconium phosphonate/carboxylate; Laccase immobilization

1. Introduction

Controlling the molecular structure and organization of the interfacial region between a solid surface and an electrolyte solution has become a matter of routine using several different chemical methods [1–3]. Among areas that have benefited from the tailoring of surface properties are bioelectrochemistry, bioelectronics, chemical and biological sensing, and bioenergetics [4–7]. The major issue and challenge in such studies is the electrical coupling of redox enzymes with electrodes, because of their possible applications as enzyme-based bioelectronic devices, e.g., biosensors or biofuel cell elements, also in nanoscale applications [8,9]. For many years it has been recognized that the enzymatic reduction of oxygen to water can be an alternative to noble metal electrocatalysis for fuel cell cathodes [10,11]. The major problem encountered is that the enzyme assemblies on electrode surfaces usually do not exhibit significant electronic communication between their redox centers and the conductive surface. This phenomenon is explained in terms of the electrical insulation of the biocatalytic redox site by the surrounding protein matrix and the improper alignment of the enzyme with respect to the electrode surface [6,7].

While redox enzymes usually do not show significant direct electron transfer with electrodes, the application of electron mediators (redox species of low molecular weight) that can shuttle electrons between the enzyme redox centers and the conductive surface is widely applied to establish electrical communication between the redox proteins and the electrodes.

Laccases (benzenediol:oxygen oxidoreductases; E.C. 1.10.3.2) are copper-containing redox enzymes that catalyze the oxidation of a broad range of polyphenols and aromatic substrates [12–14]. In contrast to widely used peroxidases, laccases are more stable, versatile and dependent only on atmospheric oxygen. These enzymes can be used effectively in bioremediation, detoxification, the pulp and paper industry and for removal of phenolic pollutants and polycyclic aromatic hydrocarbons in wastewater

* Corresponding author. Tel.: +48 22 822 02 11x389; fax: +48 22 822 59 96.
E-mail address: pakrys@chem.uw.edu.pl (P. Krysiński).

1567-5394/$ - see front matter © 2007 Elsevier B.V. All rights reserved.
doi:10.1016/j.bioelechem.2006.12.006

and soil [15–17]. Apart from their industrial use, since laccase oxidation is coupled with the reduction of dioxygen, these enzymes were also employed as a cathode "active" material in biofuel cells. The effective use of an enzyme can be enhanced by its immobilization on a solid support. This structural motif results in operational stability and durability of the enzyme with the aim of cost reduction particularly for, e.g., continuous processes or by reuse of the enzymes. Laccases were usually immobilized in porous materials like glass or clays, physically adsorbed on electrode surfaces or covalently bound to the surface, typically with glutaraldehyde or carbodiimide chemistry [18–20]. The method by which an enzyme is immobilized at an electrode surface is a critical factor in providing a flexible yet stable layer of the bioactive species in a form that maintains its native behaviour. Moreover, the surface-attachment chemistry should provide the proper orientation of an enzyme to establish efficient electronic contact between such an enzyme and the electrode surface.

We present here a simple method allowing for stable laccase immobilization on various conducting surfaces that retains the activity of the enzyme. The strategy for laccase immobilization presented in this paper relies on ionic coordination chemistry involving $-COO^-$ terminal groups present on the protein. In our previous work [21] we have used zirconium phosphate/phosphonate (ZP) chemistry, pioneered by the Mallouk [22], Thompson [23] and Katz [24] groups, to attach molecules to boron-doped diamond (BDD). As shown previously, Zr^{4+} ions coordinated to phosphonate and phosphate groups can bind carboxylate and sulfonate functionalities. This chemistry allows immobilization of carboxylic (ZPC) and sulfonic acids to zirconated phosponate/phosphate monolayers [25,26]. It has been also demonstrated that Hf^{4+} cations can also be used to bind $-COO^-$ and $-SO_3^-$ groups to phosphonate containing monolayers on the surface [27]. Therefore, this chemistry appears to be sufficiently versatile to be used for the surface modification of a variety of surfaces with redox enzymes via their terminal carboxylate groups in a way that provides sufficient flexibility of the surface binding functionality to retain the requisite bio-activity.

Using atomic force microscopy (AFM), resonance Raman scattering (RR), surface enhanced Raman scattering (SERS), surface plasmon resonance (SPR), quartz crystal microbalance (QCM) gravimetry and electrochemical techniques, we show that laccase bound to an electrode surface via zirconium phosphonate/carboxylate (ZPC) chemistry forms a relatively stable layer with the enzyme retaining its bio-activity.

2. Experimental

2.1. Materials

2.1.1. Chemicals

All chemicals were of the highest purity available commercially: 11-mercaptoundecanol (MUOH, Aldrich, 97%), dodecanethiol (Aldrich), phosphorus oxychloride $POCl_3$ (Merck, 99%), zirconyl chloride octahydrate (Merck), 2,4,6-collidine (Aldrich, 99%), syringaldazine (4-hydroxy-3,5-dimethoxybenzaldehyde azine) (Aldrich, 99%), syringic acid (Fluka, 97%) 2,6-dimethoxyphenol (2,6-DMP, Aldrich, 99%), ethanol (Chempur) and acetonitrile (Aldrich, anhydrous, 99.8%) were used in this work. Aqueous solutions were prepared with MilliQ water.

2.2. Source of laccase

Laccase was obtained from *Cerrena unicolor* (C-139) fungus according to a procedure that has been reported previously [18]. The post-culture liquid containing laccase was centrifuged at 10,000 ×*g*, and concentrated using an ultrafiltration system with a Pellicon 2 Mini holder (Millipore, Bedford, MA, USA) with an Ultracel mini cartridge (10 kDa cut off). The resulting crude enzyme was purified on a DEAE-Sepharose column pre-equilibrated with 20 mM Tris®-HCl buffer (pH 6.5) with 0.1 M NaCl and proteins were eluted with a 0.1–0.5 M linear gradient of NaCl at a flow rate of 1 mL/min. The concentration of isolated and frozen (−18 °C) enzyme was $c_{lacc} = 178$ μg cm^{-3} and its activity was 186,000 nkat dm^{-3}.

2.3. Determination of laccase activity

Enzyme activity was measured spectrophotometrically with syringaldazine as the substrate for laccase [28]. The protein content was determined according to Bradford with bovine albumin as the standard [29]. The activity of the immobilized laccase was measured using polarographic analysis with a Clark-type oxygen electrode (Rank, Cambridge, UK) [30]. The reaction mixture was stirred at 120 rpm.

2.4. Methods

2.4.1. Raman and SERS spectroscopy

Raman spectra were recorded with a Jobin Yvon Spex T64000 Raman microscope equipped with a Kaiser holographic notch filter, a 600 groove mm^{-1} holographic grating, and a 1024×256 pixel liquid nitrogen cooled CCD detector. The microscope attachment was based on an Olympus BX system with a 50× long working distance objective. The excitation source was a Laser-Tech model LJ-800 mixed argon–krypton ion laser operating at wavelengths of 514.5 nm and 647.1 nm. A band-pass filter (Coherent model 35-8663 (647.1 nm) or model 35-8424 (514.5 nm)) was placed in the laser beam prior to the sample. The sample was irradiated with ca. 10 mW average power from the laser.

2.4.2. Tapping mode atomic force microscopy (TM AFM)

Atomic Force Microscopy operating in tapping mode was performed using Digital Instruments Nanoscope IIIa (Veeco). The measurements were performed *ex-situ* in air, using etched silicon probes.

2.4.3. Surface plasmon resonance (SPR)

Surface plasmon resonance experiments were carried out with an Autolab Esprit/Springle system (Eco Chemie B.V., The Netherlands) operating at fixed 670 nm wavelength, with gold coated glass disks provided by the manufacturer as SPR

sensors. The sensor surface was modified as described below, placed in the SPR cuvette with the sample loading/injection system and used for further *in-situ* experiments, where the resonance minimum was recorded vs. the angle of laser beam reflected from gold.

2.4.4. Quartz crystal microbalance (QCM)

QCM measurements were made using a quartz crystal microbalance module of the KSP electrochemical workstation and AT-cut (10 MHz) quartz crystals having 100 nm thick evaporated gold electrodes (International Crystal Mfg., Oklahoma City, USA) with a surface area of 0.21 cm^2. The mass of the surface-bound species was calculated using the Sauerbrey equation.

2.4.5. Clark-type oxygen electrode

A Clark-type oxygen electrode (Rank, Cambridge, Great Britain) connected to a linear TZ 4100 recorder (Laboratorni Pristroje, Praha, Czech) was used for determination of oxygen concentration.

2.5. Substrate preparation and modification

Different substrates, depending upon the experimental technique used were prepared and their surface modified in order to enable the enzyme attachment. These are listed below.

2.5.1. Indium-doped tin oxide

ITO films (sheet resistance, R_s 5–15 Ohm, Delta Technol., Ltd., USA) deposited on glass slides (Delta Technologies) were cleaned by rinsing with ethanol and dried prior to use.

2.5.2. Polycrystalline gold substrates for electrochemical measurements and QCM crystals

Evaporated gold substrates used for electrochemical measurements and as electrodes for QCM measurements were made with evaporated gold and were electrochemically cleaned by cyclic scanning in 0.1 M H_2SO_4 within the potential range −300–+1500 mV vs. Ag,AgCl/1M KCl_{aq} electrode, (scan rate 100 mV/s) as described earlier [31,32], until stable cyclic voltammetric curves characteristic of clean polycrystalline gold were obtained [33].

2.5.3. Gold substrates for AFM measurements

For AFM measurements, the substrates used were glass slides covered with ca. 250 nm of evaporated Au(111) (Arrandee, Germany). The gold-coated substrates were annealed in the flame of a Bunsen burner for a brief period (several seconds) prior to use.

2.5.4. Gold and silver substrates for Raman and SERS

For SERS experiments the silver electrodes were roughened in a separate electrochemical cell by three successive positive–negative cycles in 0.1 M KCl aqueous solution from −0.3 to 0.3 V (vs. a Ag/AgCl electrode in 0.1 M KCl) at a sweep rate of 5 mV/s. The roughening procedure for gold electrodes consisted of 20 oxidation–reduction cycles between −0.6 and +1.2 V vs the same reference electrode at a sweep rate of 500 mV/s in 0.1 M KCl, pausing at −0.6 V for 8 s and at +1.2 V for 3 s. Finally, the roughened gold electrode was held at −0.6 V for 5 min. The working silver and gold electrodes were removed at an open circuit potential, rinsed carefully with distilled water and dried.

All gold and silver substrates were exposed to a chloroform solution containing 2 mg/mL of 11-mercaptoundecanol for 60 min to produce a hydroxyl-terminated monolayer.

Surface-modified gold and silver, as well as cleaned ITO substrates were reacted with phosphorus oxychloride (0.3 mL) in dry acetonitrile (10 mL), using 2,4,6-collidine (0.3 mL) as a catalyst, under reduced pressure. After 30 min, the substrates were removed, rinsed with reagent grade acetonitrile and then water and zirconated by immersion for 30 min in 5 mM $ZrOCl_2$ in 60% aqueous ethanol. The resulting zirconated substrates were exposed to a solution containing laccase for 30 min. The reacted substrates were removed from the reaction vessel, washed with water and used immediately in the experiments reported below. For the TM-AFM experiments, the substrates were dried with a stream of air prior to use.

2.5.5. Measurement of laccase kinetics

In order to determine the kinetics of immobilized *C. unicolor* laccase, the activated ITO slides (2.5 cm^2) and Au-coated glass slides (1.21 cm^2, Arrandee, Germany) were incubated at 20 °C with 0.5 mg of laccase protein dissolved in 0.1 M acetic buffer pH 5.0 (5 mL) in a rotary shaker (30 rpm) for 5 h. Next, the slides (ITO and Au) coated with attached laccase were washed three times with 15 mL portions of Milli Q water and used for the determination of laccase kinetics.

3. Results and discussion

3.1. SPR and QCM of laccase deposition

SPR measurements allow real-time measurements of the binding of proteins or other molecules to a surface [34–37]. In our work, the gold surfaces were modified as described above, with a zirconated layer of $MUOPO_3^{2-}$ Zr^{4+} (11-mercaptoundecanol

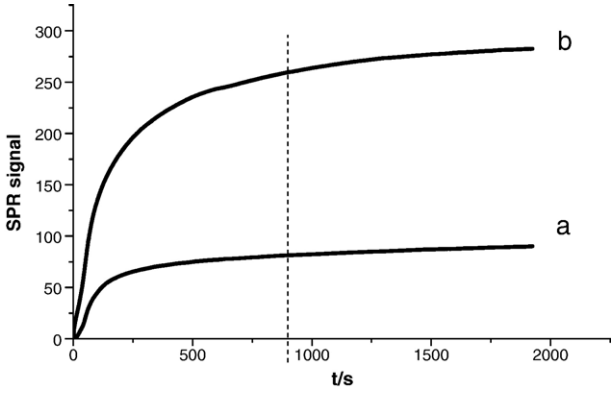

Fig. 1. SPR signal vs. time for: a) Au covered with $C_{12}SH$ SAM in the presence of aqueous solution of laccase, b) Au covered with ZP layer in the presence of aqueous solution of laccase.

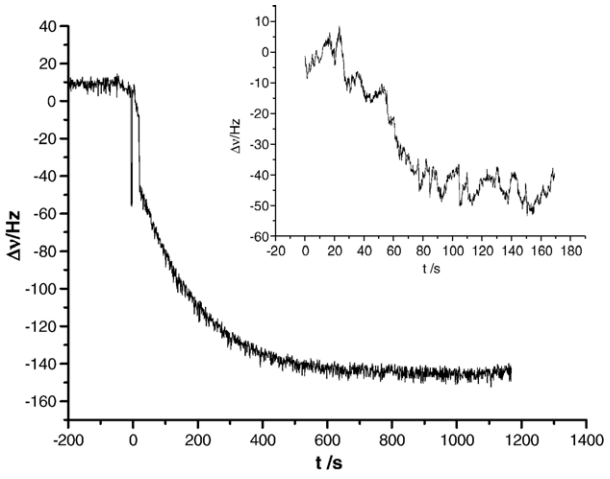

Fig. 2. QCM frequency change for Au covered with ZP layer in the presence of aqueous solution of laccase. This corresponds to ca. 8.0×10^{-12} mol/cm^2 laccase (assuming 65 kDa). Insert shows the frequency change upon modification of Au surface with MUOH.

monolayer on gold, derivatised with OPO_3^{2-} groups and capped with Zr^{4+} ions), and a shift in the surface plasmon resonance angle vs. time was measured as a function of time after 200 μL of laccase solution in water (0.50 mg/mL) was added to the SPR cuvette (Fig. 1). For comparison, similar experiments were carried out for gold films modified with n-mercaptododecane, a surface that presents hydrophobic methyl groups to the laccase-containing solution. As can be seen from Fig. 1a and b, both the amount and kinetics of laccase deposition differ significantly for the two modified surfaces. The relationship between SPR angle change and the amount of bound dielectric is linear. Generally speaking, a change in protein surface mass density of 1 ng/mm^2 corresponds to a shift in SPR angle of ca. 120 mdeg (assuming a refractive index for the adsorbed dielectric layer of 1.4). This proportionality yields a surface coverage of ca. 2.3×10^{-7} g/cm^2 for our substrates modified using ZPC chemistry and 0.7×10^{-7} g/cm^2 for the dodecanethiol-modified gold substrates.

We have also monitored the formation of the ZPC-bound laccase adlayer by means of QCM gravimetry. We show in Fig. 2 the time-dependent QCM resonance frequency decrease with laccase deposition. The inset shows the frequency change with formation of 11-mercaptoundecanol monolayer as the first step in the preparation of the surface. The frequency change was converted to the mass of the deposited laccase using the Sauerbrey equation, yielding 5.2×10^{-7} g/cm^2 of laccase on gold. This value is higher than that obtained from the SPR measurements (2.3×10^{-7} g/cm^2), and we understand this difference in the context of the different quantities measured by the two techniques. For the QCM measurements, we sense the total mass deposited on the sensor crystal, including both the mass of the laccase adlayer and the water dynamically coupled to the protein, while for SPR measurements, the value obtained is solely that of the adsorbed protein film [37,38]. Assuming that the average molecular mass of the laccase unit is 65 kDa, the surface coverage can be estimated as 8.0×10^{-12} mol/cm^2 (QCM) and 3.5×10^{-12} mol/cm^2 (SPR).

3.2. AFM of laccase deposited on gold

The deposition of laccase onto gold surface was confirmed by Tapping Mode AFM measurements. The tapping mode of operation was chosen in order to reduce lateral forces exerted by the tip on the sample [39].

We show in Fig. 3 the AFM image and a cross section through a gold surface modified with laccase. In this image, there are a number of globular structures scattered uniformly on the surface. It should be stressed here, that such features are not

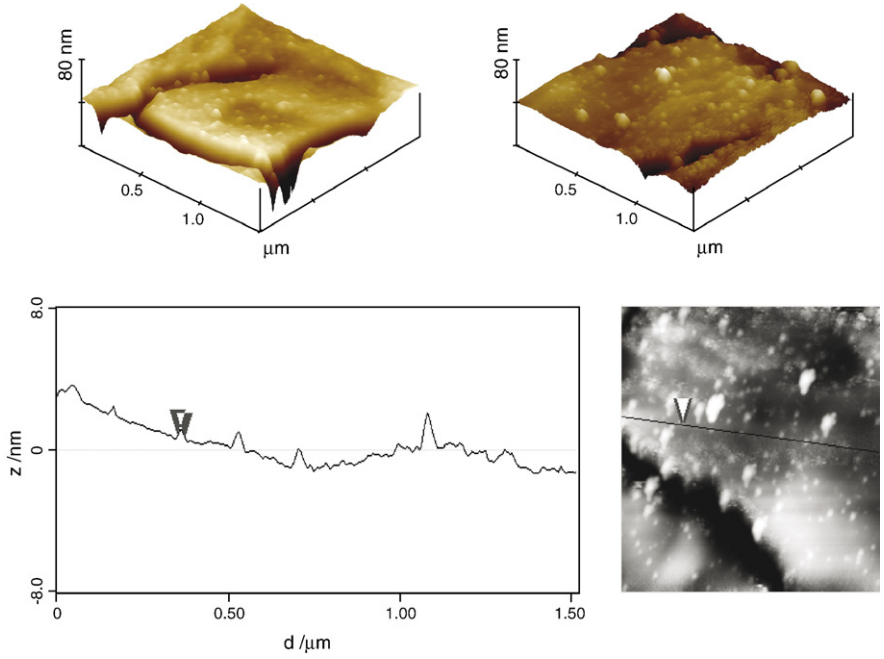

Fig. 3. TM AFM image and a cross-section through the gold surface modified with laccase.

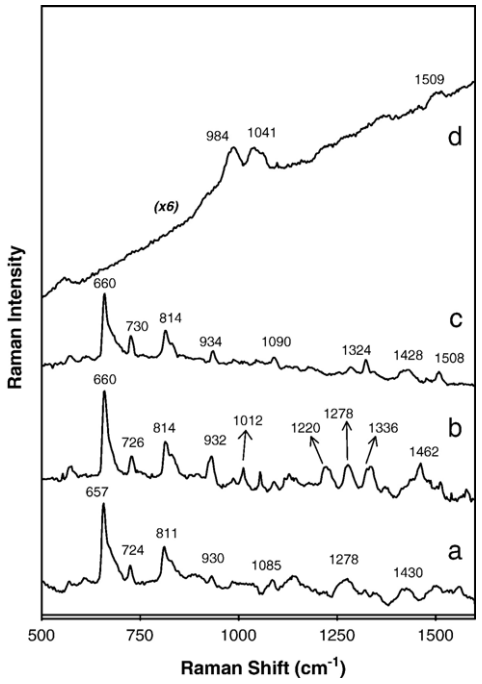

Fig. 4. Series of the SERS spectra (a–c) recorded at the Ag surface after subsequent steps of substrate modification: (a) Ag/MUOH; (b) $Ag/MuOPO_3^{2-}$; (c) $Ag/MUOPO_3^{2-}Zr^{4+}$, and resonance Raman spectrum of ethanol solution of syringaldazine in contact with $Ag/MUOPO_3^{2-}Zr^{4+}$ laccase substrate. λ_{exc}=647.1 nm for spectra (a–c) and 514.5 nm for spectrum (d).

observed on bare gold or on surfaces modified using ZP chemistry. The diameter of the globules ranges from ca. 15 nm to 150 nm. Their height is significantly smaller, ranging from ca. 0.5 nm to ca. 10 nm, respectively. We believe these structures can be attributed to single or aggregated laccase units attached to the surface (similar aggregation phenomena were reported for laccase covalently immobilized on thiol-modified gold [20]). The surface loading density (both single and aggregated) is approximately 1.5×10^{-14} mol of globules/cm^2. As the TM AFM does not provide accurate information on the size of the imaged structures due to the tip convolution effect, we believe that the true diameter of these features may be smaller. In our case the radius of the aperture of the AFM tip is approximately 10 nm. Assuming there to be further distortion associated with the AFM feedback mechanism, we speculate that the real size of the smallest laccase spots may not exceed 10 nm. The smallest features observed in our AFM images are likely attributable to single laccase units (the crystallographic diameter of laccase unit is ca. 5 nm [40]), given the measurement-related issues and the modest surface loading density, while the larger structures are probably aggregates of the protein. In fact, we also cannot exclude the possibility that together with the enzyme some organic residues are coadsorbed that cause larger aggregate size. Also the height of the protein spots determined by AFM may be influenced by the instrument itself — the protein material is extremely soft therefore it can affect vibrations of the cantilever operating in the tapping mode. Even though the exact height determination might be inaccurate it is likely that the real geometry of laccase spots is disk-like rather than spherical, especially under *ex situ* conditions.

3.3. Resonance Raman spectra of syringaldazine oxidized by laccase on Au and Ag

To find evidence of laccase immobilization by coordination to zirconium phosphate functionalities, Raman spectroscopic experiments were performed. We used surface-enhanced Raman scattering (SERS) to enhance the inherently weak Raman spectrum of the surface adlayers, in concert with the resonance Raman effect. It is well established that the highest enhancement factors in SERS are observed for molecules adsorbed or bound to roughened Ag surface. We have measured Raman spectra on both Ag and Au surfaces for this work. The SERS spectra of the molecular assemblies formed on our surfaces were recorded at each step of modification process for both the Ag and Au surfaces.

We show in Fig. 4 the Raman spectrum of a MUOH adlayer deposited on silver, revealing strong SERS enhancement. The most prominent band at 657 cm^{-1} corresponds to the C–S stretching vibration of the gauche conformer of the –S–C–C– chain [41,42]. This band is red-shifted by about 30 cm^{-1} compared to the spectrum of a powdered sample of MUOH, which exhibits two bands at 690 and 715 cm^{-1} (spectrum not shown). The band at 657 cm^{-1} seen for our surface-bound sample is strongly asymmetric on the high-frequency side indicating a rather broad distribution of torsion angles for the –S–C–C– chain. The band that could be ascribed to the trans conformer in the (unenhanced) Raman spectrum of powdered MUOH (at 715 cm^{-1}) is not observed in the SERS spectrum. These observations provide strong evidence for considerable conformational disorder near the thiol group of MUOH adsorbed on the Ag surface. After modification of the MUOH monolayer with phosphonate groups, several new bands in the

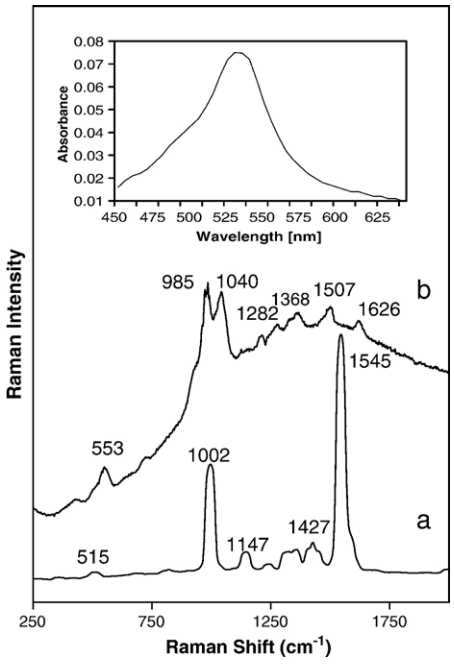

Fig. 5. Normal Raman spectrum of syringaldazine powder (a) and resonance Raman spectrum of syringaldazine solution in presence of laccase (b); λ_{exc}=514.5 nm. Inset – Visible spectrum of syringaldazine – laccase solution.

1000–1500 cm^{-1} spectral region appear in the SERS spectrum (Fig. 4b). These bands likely correspond to the vibrations of the attached OPO_3^{2-} groups. Some of them are quite intense, thus indicating that these groups are situated relatively near the Ag surface, because an electromagnetic field responsible for large increase of Raman intensity in the SERS effect quickly decays with a distance from the metal surface. The characteristic distance at which SERS signals decrease by half is about 0.7 nm [43]. However, after coordination of the Zr^{4+} ions to the phosphonate groups these new bands disappear and the spectrum exhibits exclusively the bands characteristic for MUOH (compare spectra a and c in Fig. 4). There is a possibility that the bands due to vibrations of the phosphonate groups coordinated to Zr^{4+} are shifted and weakened a lot. However, this observation may also suggest that, after the zirconation step, the–OPO_3^{2-} groups coordinated to Zr^{4+} are far away from the metal surface and Zr^{4+} cations are accessible for the–COO^- groups of the enzyme.

After immobilization of laccase at the zirconium–phosphonate terminated surface the Raman spectrum remained essentially unchanged (spectrum not shown). We have recently developed a new, indirect method of monitoring laccase immobilized on thiol-coated Ag and Au surfaces [44]. In this method we record the resonance Raman (RR) spectra (laser excitation at 514.5 nm) of the coloured product (red) of the oxidation of syringaldazine (4-hydroxy-3,5-dimethoxybenzaldehyde azine) by laccase in the presence of molecular oxygen. The absorption spectrum of the oxidized form of syringaldazine exhibits a prominent band with a maximum at ca. 530 nm (Fig. 5 inset). Excitation at 514.5 nm thus provides resonance enhancement for Raman scattering of this molecule. As can be seen in Fig. 5b, the RR spectrum of the oxidation product of syringaldazine in the solution exhibits characteristic bands at 985 and about 1040 cm^{-1} in addition to several weaker bands superimposed on a broad fluorescence background. We have not made definitive assignments for these bands at this point, however one might speculate that they are due to stretching vibrations of the N═N bonds and quinone fragment of the molecule (for respective chemical formulae see Fig. 1 in [44]). This RR spectrum is considerably different from the off-resonance Raman spectrum of a solid sample of the reduced form of syringaldazine, which are characterized by two strong bands at 1005 and 1553 cm^{-1} due to ν(N–N) and ν(C═N) of conjugated azines [45]. Therefore, to establish the presence of laccase on the zirconium phosphonate-terminated surface and to test its enzymatic activity, a 0.5 mM ethanolic solution of syringaldazine was placed on the surface bearing the immobilized enzyme and washed thoroughly with water. Subsequently, the resonance Raman spectrum of the (coloured) syringaldazine oxidation product was recorded (514.5 nm excitation, Fig. 4d). This spectrum contains the same two bands that are characteristic of oxidized syringaldazine in the solution (984 and about 1040 cm^{-1}), confirming both the presence and enzymatic activity of laccase on the modified surface. The spectrum shown in Fig. 4d is dominated by the bands of oxidized form of syringaldazine (for comparison see the spectrum b in Fig. 5). In the conditions of experiment the bands of both MUOH and laccase are hardly visible because of strong, selective resonance enhancement of the Raman bands of oxidized syringaldazine. Similar experiments were performed for the zirconium phosphonate-modified Au surface. A series of the Raman spectra recorded after each step of the surface modification is presented in Fig. 6. The SERS spectrum of the MUOH monolayer at the Au surface (Fig. 6a) is very similar to that observed for the silver support. It seems however, that the conformational disorder observed at the Ag surface is considerably smaller for MUOH monolayer on the Au support, as judging from the symmetry of the 660 cm^{-1} band ascribed to the ν(CS) vibration. Moreover, in contrast to the Ag surface, the SERS spectrum of MUOH on the Au surface remains unchanged after attachment of the $–OPO_3^{2-}$ groups (Fig. 6b). It may suggest that in this case the $–OPO_3^{2-}$ groups are far away from the metal surface. It is also possible that the Ag surface is partially oxidized — accounting for the disorder, and that there is some phosphate interaction with the AgO that cannot happen for the Au surface. The SERS spectra recorded after subsequent steps of the Au functionalisation (Fig. 6c and d) remain unchanged. Substantial changes in the Raman spectrum are seen only after exposure of the laccase-modified surface of syringaldazine (Fig. 6e). In this spectrum the 993 and 1044 cm^{-1} bands, characteristic of oxidized syringaldazine, are clearly visible, demonstrating enzyme binding and activity at the Au surface as well. With the demonstration of laccase binding and enzymatic activity, we consider in more detail the kinetics of the surface-bound enzyme.

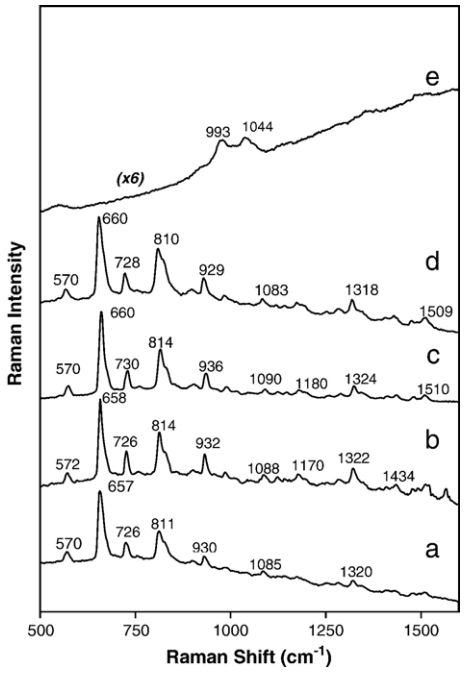

Fig. 6. Series of the SERS spectra (a–d) recorded at the Au surface after subsequent steps of substrate modification: (a) Au/MUOH; (b) Au/$MUOPO_3^{2-}$; (c) Au/$MUOPO_3$ $^{2-}Zr^{4+}$; (d) Au/$MUOPO_3$ $^{2-}Zr^{4+}$ laccase; (e) resonance Raman spectrum of ethanol solution of syringaldazine in contact with Au/$MUOPO_3$ $^{2-}Zr^{4+}$ laccase substrate. λ_{exc}=647.1 nm for spectra (a–d) and 514.5 nm for spectrum (e).

Table 1
Kinetic data of native and immobilized laccases of *Cerrena unicolor*

Substrate	Native laccase	Laccase immobilized on ITO	Laccase immobilized on Au
	K_m [mM]	K_m [mM]	K_m [mM]
2,6 DMP	0.08±0.01	0.45±0.01	0.79±0.04
Syringic acid	0.07±0.01	0.43±0.03	0.71±0.05

3.4. Enzyme kinetics

The Michaelis–Menten approach applied to the activity of free and immobilized laccase as a function of 2,6-dimethoxyphenol (2,6-DMP) and syringic acid (3,5-dimethoxy-4-hydroxy benzoic acid) concentrations indicates that the immobilization process strongly affects the kinetic parameters of the enzyme (Table 1). The higher K_m (Michaelis constant) values for the immobilized laccase indicate lower affinity for the substrate after immobilization. The effect of surface confinement on the kinetic behaviour of bound enzymes was observed previously [45]. When the diffusion of the enzyme substrate from bulk of the solution to the bound enzyme is relatively slow as compared to the enzyme turnover, the substrate concentration is lower in the immediate environment of the enzyme than in the bulk. This results in the apparent reduction of the enzyme activity, an increase of the K_m value and is referred to as the diffusional inhibition [46,47]. On the other hand, the enzyme spatial structure and organization, particularly around the active site of the molecule, very effectively influences the activity of the enzyme. The coordination of *C. unicolor* laccase to modified ITO or gold surfaces via the carboxylic groups coming from the aspartic and glutamic acid residues should change the enzyme conformation. This effect will also cause an increase of the "apparent" K_m values. As a result the higher bulk concentration of the enzyme substrate is apparently required to reach half of the maximum reaction rate as compared to native laccase.

4. Conclusions

We have presented a simple method for stable laccase immobilization on various conducting surfaces, and the surface binding of the protein allows it to retain its enzymatic activity. The interfacial chemistry we use relies on the ionic coordination of zirconium phosphonate to carboxylate $-COO^-$ terminal groups present on the protein.

Using a host of techniques, including surface plasmon resonance (SPR), quartz crystal microbalance (QCM) gravimetry, atomic force microscopy (AFM), surface enhanced Raman scattering (SERS), resonance Raman scattering (RR) and electrochemical techniques, we show that laccase bound to a surface coordinatively through zirconium phosphonate/carboxylate (ZPC) functionalities forms a stable enzymatic layer with the enzyme retaining its activity to a significant extent.

Our enzyme kinetics data reveal that surface-immobilization of the enzyme apparently alters its bioactivity, as seen by higher K_m values. However, it is well known that the activity of enzyme immobilized on a solid substrate is strongly affected by the formation of a diffusion layer. This leads to an increase of the apparent Michaelis constant K_m being measured, suggesting sluggish than actual enzyme kinetics. Thus, at this point, the increase of K_m values observed for laccase bound either to ITO or Au surfaces can be understood in terms of conformational changes of the enzyme on the surface or higher diffusion constraint increasing the apparent K_m values.

Acknowledgements

This work was supported by the Ministry of Scientific Research and Information Technology in 2004–2007, Project No. PBZ 18-KBN098/T09/2003 and by the National Science Foundation Grant 0445492. The NSF-PAS mobility grant is also acknowledged.

References

[1] Ph. Leclère, M. Surin, R. Lazzaroni, A.F.M. Kilbinger, O. Henze, P. Jonkheijm, F. Biscarini, M. Cavallini, W.J. Feast, E.W. Meijer, A.P.H.J. Schenning, Surface-controlled self-assembly of chiral sexithiophenes, J. Mater. Chem. 14 (2004) 1959–1963.
[2] P.E. Laibnis, G.M. Whitesides, ω-Terminated alkanethiolate monolayers on surfaces of copper, silver, and gold have similar wettabilities, J. Am. Chem. Soc. 114 (1992) 1990–1995.
[3] H.-I. Kim, O. Oloba, T. Koini, S. Imaduddin, T.R. Lee, S.S. Perry, Molecularly specific studies of the frictional properties of monolayer films: a systematic comparison of CF_3-, $(CH_3)_2CH-$, and CH_3-terminated films, Langmuir 15 (1999) 3179–3185.
[4] I. Willner, E. Katz, Integration of layered redox proteins and conductive supports for bioelectronic applications, Angew. Chem., Int. Ed. 39 (2000) 1180–1218.
[5] E. Katz, I. Willner, J. Wang, Electroanalytical and bioelectroanalytical systems based on metal and semiconductor nanoparticles, Electroanalysis 16 (2004) 19–44.
[6] F.A. Armstrong, G.S. Wilson, Recent developments in faradaic bioelectrochemistry, Electrochim. Acta 45 (2000) 2623–2645.
[7] S.C. Barton, J. Gallaway, P. Atanassov, Enzymatic biofuel cells for implantable and microscale devices, Chem. Rev. 104 (2004) 4867–4886.
[8] M. Zayats, E. Katz, I. Willner, Electrical contacting of flavoenzymes and $NAD(P)^+$-dependent enzymes by reconstitution and affinity interactions on phenylboronic acid monolayers associated with Au-electrodes, J. Am. Chem. Soc. 124 (2002) 14724–14735.
[9] J. Wang, Nanomaterial-based electrochemical biosensors, Analyst 130 (2005) 421–426.
[10] A. Heller, Miniature biofuell cell, Phys. Chem. Chem. Phys. 6 (2004) 209–216.
[11] N. Mano, H.-H. Kim, A. Heller, On the relationship between the characteristics of bilirubin oxidases and O_2 cathodes, J. Phys. Chem. 106 (2002) 8842–8848.
[12] E.I. Solomon, U.M. Sundaram, T.E. Machonkin, Multicopper oxidases and oxygenases, Chem. Rev. 96 (1996) 2563–2605.
[13] J. Rogalski, A. Leonowicz, Production and application of laccase, in: A. Pandey (Ed.), Concise Encyclopedia of Bioresource Technology, The Haworth Press, Inc., Binghamton, USA, 2004, pp. 533–542.
[14] N. Durán, M.A. Rosa, A. D'Annibale, L. Gianfreda, Applications of laccases and tyrosinases (phenoloxidases) immobilized on different supports: a review, Enzyme Microb. Technol. 31 (2002) 907–931.
[15] R.P. Chandra, A.J. Ragauskas, Biotechnology in the pulp and paper industry, in: L. Viikari, R. Lantto (Eds.), Progress in Biotechnology, vol. 21, Elsevier, New York, 2002, pp. 165–172.
[16] W.R. Kenealy, T.W. Jeffries, Enzyme processes for pulp and paper: a review of recent developments, in: B. Goodell, D.D. Nicholas, T.P. Schulz (Eds.), Wood deterioration and preservation — advances in our changing world, American Chemical Society, Washington, 2003, pp. 210–239.

[17] A.M. Mayer, R.C. Staples, Laccase: new function for an old enzyme, Phytochemistry 60 (2002) 551–565.
[18] J. Rogalski, A. Dawidowicz, E. Jóźwik, A. Leonowicz, Immobilization of laccase from *Cerrena unicolor* on controlled porosity glass, J. Mol. Catal. 6 (1999) 29–39.
[19] M.-Y. Ahn, J. Dec, J.-E. Kim, J.-M. Bollag, Treatment of 2,4-dichlorophenol polluted soil with free and immobilized laccase, Environ. Qual. 31 (2001) 1509–1515.
[20] J.F. Cabrita, L.M. Abrantes, A.S. Viana, *N*-hydroxysuccinimide-terminated self-assembled monolayers on gold for biomolecules immobilization, Electrochim. Acta 50 (2005) 2117–2124.
[21] M. Mazur, P. Krysinski, G.J. Blanchard, Use of zirconium–phosphate–carbonate chemistry to immobilize polycyclic aromatic hydrocarbons on boron-doped diamond, Langmuir 21 (2005) 8802–8808.
[22] H. Lee, L.J. Kepley, H.G. Hong, S. Akhter, T.E. Mallouk, Adsorption of ordered zirconium phosphonate multilayer films on silicon and gold surfaces, J. Phys. Chem. 92 (1988) 2597–2601.
[23] L.A. Vermeulen, M.E. Thompson, Stable photoinduced charge separation in layered viologen compounds, Nature 358 (1992) 656–658.
[24] H.E. Katz, G. Scheller, T.M. Putvinski, M.L. Schilling, W.L. Wilson, C.E.D. Chidsey, Polar orientation of dyes in robust multilayers by zirconium phosphate–phosphonate interlayers, Science 254 (1991) 1485–1487.
[25] S.B. Bakiamoh, G.J. Blanchard, Demonstration of oriented multilayers through asymmetric metal coordination chemistry, Langmuir 15 (1999) 6379–6385.
[26] S.B. Bakiamoh, G.J. Blanchard, Surface second harmonic generation from asymmetric multilayer assemblies: gaining insight into layer-dependent order, Langmuir 17 (2001) 3438–3446.
[27] C.T. Buscher, D. McBranch, D. Li, Understanding the relationship between surface coverage and molecular orientation in polar self-assembled monolayers, J. Am. Chem. Soc. 118 (1996) 2950–2953.
[28] A. Leonowicz, K. Grzywnowicz, Quantitative estimation of laccase forms in some white-rot fungi using syringaldazine as a substrate, Enzyme Microb. Technol. 3 (1981) 55–58.
[29] M.M. Bradford, A rapid and sensitive method for the quantitation of microgram quantities of the protein utilizing the principle of protein-dye binding, Anal. Biochem. 72 (1976) 248–254.
[30] J. Rogalski, M. Wojtas-Wasilewska, R. Apalovic, A. Leonowicz, Affinity chromatography as a rapid and convenient method for purification of fungal laccase, Biotechnol. Bioeng. 37 (1991) 770–777.
[31] M. Domińska, K. Jackowska, P. Krysiński, G.J. Blanchard, Probing interfacial organization in surface monolayers using tethered pyrene. 1. Structural mediation of electron and proton access to adsorbates, J. Phys. Chem., B 109 (2005) 15812–15821.
[32] P. Krysiński, M. Brzostowska-Smolska, Three-probe voltammetric characterisation of octadecanethiol self-assembled monolayer integrity on gold electrodes, J. Electroanal. Chem. 424 (1997) 61–67.
[33] A. Tymosiak-Zielińska, Z. Borkowska, Interfacial properties of polycrystalline gold electrodes in tetraalkylammonium electrolytes, Electrochim. Acta 46 (2001) 3073–3082.
[34] L.S. Jung, C.T. Campbell, T.M. Chinowsky, M.N. Mar, S.S. Yee, Quantitative interpretation of the response of surface plasmon resonance sensors to adsorbed films, Langmuir 14 (1998) 5636–5648.
[35] D.D. Schlereth, Characterization of protein monolayers by surface plasmon resonance combined with cyclic voltammetry “in situ”, J. Electroanal. Chem. 464 (1999) 198–207.
[36] S. Liu, M.M.L.M. Vareiro, S. Fraser, A.T.A. Jenkins, Control of attachment of bovine serum albumin to pulse plasma-polymerized maleic anhydride by variation of pulse conditions, Langmuir 21 (2005) 8572–8575.
[37] E. Reimhult, C. Larsson, B. Kasemo, F. Höök, Simultaneous surface plasmon resonance and quartz crystal microbalance with dissipation monitoring measurements of biomolecular adsorption events involving structural transformations and variations in coupled water, Anal. Chem. 76 (2004) 7211–7220.
[38] C. Larsson, M. Rodahl, F. Höök, Characterization of DNA immobilization and subsequent hybridization on a 2D arrangement of streptavidin on a biotin-modified lipid bilayer supported on SiO2, Anal. Chem. 75 (2003) 5080–5087.
[39] D. Mayer, K. Ataka, J. Heberle, A. Offenhäuser, Scanning probe microscopic studies of the oriented attachment and membrane reconstitution of cytochrome *c* oxidase to a gold electrode, Langmuir 21 (2005) 8580–8583.
[40] V.A. Bogdanovskaya, M.R. Tarasevich, L.N. Kuznetsova, M.F. Reznik, E.V. Kasatkin, Peculiarities of direct bioelectrocatalysis by laccase in aqueous–nonaqueous mixtures, Biosens. Bioelectron. 17 (2002) 945–951.
[41] M.H. Schoenfisch, J.E. Pemberton, Effects of electrolyte and potential on the in situ structure of alkanethiol self-assembled monolayers on silver, Langmuir 15 (1999) 509–517.
[42] A. Kudelski, Structures of monolayers formed from different HS–$(CH_2)_2$–X thiols on gold, silver and copper: comparative studies by surface-enhanced Raman scattering, J. Raman Spectrosc. 34 (2003) 853–862.
[43] Q. Ye, J. Fang, L. Sun, Surface-enhanced Raman scattering from functionalized self-assembled monolayers. 2. Distance dependence of enhanced Raman scattering from an azobenzene terminal group, J. Phys. Chem., B 101 (1997) 8221–8224.
[44] A. Michota-Kaminska, B. Wrzosek, J. Bukowska, Resonance Raman evidence of immobilization of laccase on self-assembled monolayers of thiols on Ag and Au surfaces, Appl. Spectrosc. 60 (2006) 752–757.
[45] J.-M. Engasser, C. Horvath, Electrostatic effects on the kinetics of bound enzymes, Biochem. J. 145 (1975) 431–435.
[46] J.-M. Engasser, C. Horvath, Inhibition of bound enzymes. I. Antieenergistic interaction of chemical and diffusional inhibition, Biochemistry 13 (1974) 3845–3849.
[47] J.-M. Engasser, C. Horvath, Inhibition of bound enzymes. III. Diffusion enhanced regulatory effect with substrate inhibition, Biochemistry 13 (1974) 3855–3859.